Acta Pharmacologica Sinica

www.nature.com/aps

ARTICLE

EPSTI1 promotes monocyte adhesion to endothelial cells in vitro via upregulating VCAM-1 and ICAM-1 expression

Yan-rou Bei[1], Shun-chi Zhang[2], Yu Song[3], Mao-lin Tang[3], Ke-lan Zhang[3], Min Jiang[3], Run-chao He[3], Shao-guo Wu[2], Xue-hui Liu[1,2], Li-mei Wu[2], Xiao-yan Dai[4] and Yan-wei Hu[1,3]

Atherosclerosis is a chronic inflammatory disease of arterial wall, and circulating monocyte adhesion to endothelial cells is a crucial step in the pathogenesis of atherosclerosis. Epithelial-stromal interaction 1 (EPSTI1) is a novel gene, which is dramatically induced by epithelial-stromal interaction in human breast cancer. EPSTI1 expression is not only restricted to the breast but also in other normal tissues. In this study we investigated the role of EPSTI1 in monocyte-endothelial cell adhesion and its expression pattern in atherosclerotic plaques. We showed that EPSTI1 was dramatically upregulated in human and mouse atherosclerotic plaques when compared with normal arteries. In addition, the expression of EPSTI1 in endothelial cells of human and mouse atherosclerotic plaques is significantly higher than that of the normal arteries. Furthermore, we demonstrated that EPSTI1 promoted human monocytic THP-1 cell adhesion to human umbilical vein endothelial cells (HUVECs) via upregulating VCAM-1 and ICAM-1 expression in HUVECs. Treatment with LPS (100, 500, 1000 ng/mL) induced EPSTI1 expression in HUVECs at both mRNA and protein levels in a dose- and time-dependent manner. Knockdown of EPSTI1 significantly inhibited LPS-induced monocyte-endothelial cell adhesion via downregulation of VCAM-1 and ICAM-1. Moreover, we revealed that LPS induced EPSTI1 expression through p65 nuclear translocation. Thus, we conclude that EPSTI1 promotes THP-1 cell adhesion to endothelial cells by upregulating VCAM-1 and ICAM-1 expression, implying its potential role in the development of atherosclerosis.

Keywords: atherosclerosis; EPSTI1; monocyte-endothelial cell adhesion; VCAM-1; ICAM-1; p65

Acta Pharmacologica Sinica (2023) 44:71–80; https://doi.org/10.1038/s41401-022-00923-5

INTRODUCTION

Atherosclerosis is the primary pathological foundation of life-threatening cardiovascular diseases, including myocardial infarction and stroke [1]. It is a chronic inflammatory disease and mainly involves large and medium-sized arteries, characterized by endothelial dysfunction, inflammatory cell recruitment, vascular smooth muscle cell migration and proliferation, as well as extracellular lipid and fibrous tissue deposition, consequently contributing to the formation of atherosclerotic plaque [2]. Endothelial dysfunction is a crucial step in the initiation of atherosclerosis [3, 4]. The phenotypic characteristics of endothelial dysfunction include upregulation of cellular adhesion molecules, such as intercellular adhesion molecule-1 (ICAM-1) and vascular cell adhesion molecule-1 (VCAM-1), which recruit circulating monocyte to vascular walls [5, 6]. Increasing studies have revealed that the enhanced adhesion and migration of circulating monocyte to vascular endothelial cells are typical features of the inflammatory response during atherosclerosis formation [3, 7, 8]. However, the mechanism by which monocyte in circulating blood are recruited and firmly adhere to vascular endothelial cells has not been fully clarified.

Epithelial-stromal interaction 1 (EPSTI1), located on chromosome 13q13.3, was initially identified as a novel gene, which is dramatically induced by epithelial-stromal interaction in human breast cancer [9]. It has been predicted that EPSTI1 protein has 307 amino acids and a molecular mass of 35.4 kDa [9]. EPSTI1 expression is not only restricted to the breast but also in other normal tissues, including the spleen, small intestine, salivary glands, testes, germinal centers of lymph nodes, and placenta [9–11]. The role of EPSTI1 in cancer malignancy has been well studied [12–14]. Recently, the role of EPSTI1 in the immune response has received increasing attention. For example, EPSTI1 has been revealed to be upregulated in the peripheral blood cells of patients with systemic lupus erythematosus and histiocytic necrotizing lymphadenitis [15]. In addition, Kim et al. observed that EPSTI1 was highly expressed in macrophages exposed to interferon-γ and lipopolysaccharide (LPS) and could function as a modulator of macrophage activation and polarization [11]. Also, EPSTI1 was revealed to be associated with abnormal B-cell activation in primary Sjogren syndrome [16]. Although EPSTI1 is known to promote inflammatory response and be involved in autoimmune diseases, the effect of EPSTI1 on the adhesion of

[1]Laboratory Medicine Center, Nanfang Hospital, Southern Medical University, Guangzhou 510515, China; [2]Department of Clinical Laboratory, Guangzhou Twelfth People's Hospital, Guangzhou Medical University, Guangzhou 510620, China; [3]Department of Clinical Laboratory, Guangzhou Women & Children Medical Center, Guangzhou Medical University, Guangzhou 510620, China and [4]Key Laboratory of Molecular Target & Clinical Pharmacology and the State Key Laboratory of Respiratory Disease, School of Pharmaceutical Sciences, Guangzhou Medical University, Guangzhou 511436, China
Correspondence: Yan-wei Hu (ywhu0618@163.com) or Xiao-yan Dai (xdai@gzhmu.edu.cn)
These authors contributed equally: Yan-rou Bei, Shun-chi Zhang

Received: 25 January 2022 Accepted: 21 May 2022
Published online: 1 July 2022

circulating monocyte to vascular endothelial cells and its implication in atherosclerosis remain unexplored.

In this study, we report that EPSTI1 is significantly upregulated in human atherosclerotic plaques versus normal arteries. Furthermore, the expression of EPSTI1 in endothelial cells of human and mouse atherosclerotic plaques is higher than that of the normal arteries. EPSTI1 elevates VCAM-1 and ICAM-1 mRNA and protein levels, resulting in increased THP-1 cell adhesion to endothelial cells. Additional, LPS-induced VCAM-1 and ICAM-1 expression and subsequent THP-1-endothelial cell adhesion are abrogated by EPSTI1 loss. Mechanistically, we demonstrated that LPS positively regulates the EPSTI1 level in a p65-dependent manner. Our results reveal a previously undescribed role of EPSTI1 in monocyte-endothelial cell adhesion and suggest its potential implication in atherosclerosis.

MATERIALS AND METHODS

Subjects

Atherosclerotic arterial samples were collected from patients undergoing carotid endarterectomy or abdominal aorta surgery at Nanfang Hospital. Arteries without macroscopic evidence of atherosclerosis were collected from individuals who died either in a road traffic accident or due to cerebral edema. The tissue samples collected were snap-frozen in liquid nitrogen before the analyses of this study. The study was approved by the Committee for Ethical Review of Research Involving Human Subjects, Southern Medical University. Informed consent was obtained from the participants or relatives of deceased individuals.

Animals and treatments

Male 8-week-old ApoE$^{-/-}$ mice were purchased from Beijing HFK Bioscience Company (Beijing, China). ApoE$^{-/-}$ mice were randomly divided into normal diet group and Western diet group. A Western diet (0.15% cholesterol and 21% fat) was obtained from Guangdong Medical Laboratory Animal Center. All mice were fed for 12 weeks, given ad libitum access to water, and kept on a 12-h light-dark cycle. All animal experiments were approved by the Animal Research Ethics Committees of Guangzhou Medical University. Animal care and use were performed in accordance with the National Institutes of Health Guide for the Care and Use of Laboratory Animals.

Cell culture

Primary human umbilical vein endothelial cells (HUVECs) were purchased from the American Type Culture Collection (ATCC) (PCS-100-010; Manassas, VA, USA) and cultured in endothelial cell culture medium (ECM) (1001; ScienCell, Carlsbad, CA, USA) supplemented with 15% fetal bovine serum (FBS) (10091-148; Gibco, Gaithersburg, MD, USA). HUVECs from passages 4–6 were used in the following experiments. HUVECs were grown to 80% confluence before treatment with 0, 100, 500, or 1000 ng/mL of LPS (tlrl-smlps; InvivoGen, San Diego, CA, USA) or 500 ng/mL LPS for 0, 6, 12, or 24 h. THP-1 (human monocyte) cells (TIB-202; ATCC) were cultured in RPMI-1640 medium (22409; Gibco) supplemented with 10% FBS. Cells were seeded in 6- or 12-well plates and 60 mm dishes and incubated in a 5% CO_2 atmosphere at 37 °C.

Preparation of LPS solution

LPS dry powder was dissolved according to the manufacturer's instructions. Stock LPS solution was made using 5 mg dry powder added to 1 mL phosphate-buffered saline (PBS), and then diluted according to the needs of the experiment.

Real-time quantitative PCR (qPCR)

Total RNA was extracted using TRIzol reagent (21101; Accurate Biology, Changsha, China) following the instructions of the manufacturer. The concentration and purity of RNAs were measured using a NanoDrop One instrument (Thermo Fisher Scientific, Waltham, MA, USA). Then, a Reverse Transcription Kit (11706; Accurate Biology) was used to synthesize cDNA. The expression levels were evaluated using a LightCycler® 480 Instrument II (Roche, Basel, Switzerland) using a SYBR Green real-time PCR premix kit (11701; Accurate Biology). The primers used are listed in Table 1.

Table 1. DNA sequence of all used primer pairs.

Gene	Sequence (5′-3′)
GAPDH-F	GCACCGTCAAGGCTGAGAAC
GAPDH-R	TGGTGAAGACGCCAGTGGA
EPSTI1-F	ACTGGCTTCTCCTTGTCCTCATTTATG
EPSTI1-R	AATGTAGCATTTCCCTGGCAGTAGAG
VCAM-1-F	TCTCATTGACTTGCAGCACCACAG
VCAM-1-R	CCTCATTCGTCACCTTCCCATTCAG
ICAM-1-F	GGTAGCAGCCGCAGTCATAATGG
ICAM-1-R	GTGGCTTGTGTGTTCGGTTTCATG
p65-F	TGGGAATCCAGTGTGTGAAGAAGC
p65-R	CCGCACAGCATTCAGGTCGTAG

Western blot

Total protein was extracted with RIPA buffer (FD008; Fdbio Science, Hangzhou, China) added with protease inhibitor cocktail (HY-K0010; MedChemExpress, Monmouth Junction, NJ, USA). Nuclear and cytoplasmic protein were extracted by using Nuclear and Cytoplasmic Protein Extraction Kit (20126ES50; Yeasen, Shanghai, China). Protein concentrations were measured using the BCA protein assay (P0012; Beyotime, Shanghai, China). Protein samples were separated using 10%–12% SDS-PAGE and transferred to nitrocellulose blotting membranes (P-N66485; Pall, Port Washington, NY, USA). Membranes were blocked with 5% skimmed milk (232100; BD-Biosciences, San Jose, CA, USA) in TBS-T (20 mM Tris-HCl, pH 7.4, 150 mM NaCl, and 0.1% Tween 20) for 1 h at room temperature, and then incubated with the appropriate primary and secondary antibodies. The primary antibodies were as follows: rabbit anti-EPSTI1 antibody (11627-1-AP, 1:1000 dilution; Proteintech, Rosemont, IL, USA), rabbit anti-VCAM-1 antibody (ab134047, 1:1000 dilution; Abcam, Cambridge, UK), rabbit anti-ICAM-1 antibody (ab282575, 1:1000 dilution; Abcam), rabbit anti-p65 antibody (8242, 1:1,000 dilution; Cell Signaling Technology, Danvers, MA, USA), rabbit anti-phospho-p65 antibody (Ser536) (3033, 1:1000 dilution; Cell Signaling Technology), and mouse-anti-GAPDH antibody (sc-1371791, 1:5000 dilution; Santa Cruz Biotechnology, Santa Cruz, CA, USA). The immunoblot signals were detected using an Amersham™ Imager 600 (GE Healthcare, Chicago, IL, USA) and the intensities of the protein bands were semi-quantitatively analyzed using ImageJ software (National Institutes of Health, Bethesda, MD, USA).

Transfection with small interfering RNA (siRNA) and plasmids

The siRNAs against EPSTI1 (siEPSTI1), VCAM-1 (siVCAM-1), ICAM-1 (siICAM-1), p65 (sip65), and an irrelevant 21-nucleotide control siRNA (negative control, siNC) were purchased from Ribo Biotechnology (Guangzhou, China). The siRNA sequences are listed in Table 2. Two plasmids containing EPSTI1 and p65 full-length cDNA were constructed by Tsingke Biotechnology (Beijing, China) and named pcDNA3.0-EPSTI1 and pcDNA3.0-p65, while the empty vector, pcDNA-3.0, served as a negative control. Electrophoresis and sequencing were then performed. HUVECs (2×10^6 cells/well) were transfected with jetPRIME® transfection reagent (114-15; Yeasen) according to the manufacturer's instructions. The qPCR and Western blot analysis were performed after 24–48 h of transfection to verify the transfection efficiency.

Table 2. The siRNA sequences used in the study.

Gene	Sequence (5′-3′)
si-EPSTI1 #1	CCGCTGAGTTCTGAGCAA
si-EPSTI1 #2	GTCAGAAACTGAAGTCAGA
siEPSTI1 #3	ACACCTTGATAGCACCAAA
siVCAM-1 #1	GGATAATCCTGAAGAAAAA
siVCAM-1 #2	GGAAGTCCCTGGAAACCAA
siVCAM-1 #3	GGCTCACAATTAAGAAGTT
siICAM-1 #1	GCAAGAAGATAGCCAACCA
siICAM-1 #2	CCAACGTGATTCTGACGAA
siICAM-1 #3	GACTGTCACTCGAGATCTT
sip65 #1	GATTGAGGAGAAACGTAAA
sip65 #2	CCCACGAGCTTGTAGGAAA
sip65 #3	GCATCCAGACCAACAACAA

Monocyte adhesion assay
THP-1 cells were suspended in serum-free medium (1×10^6 cells/mL) and stained with Dil (C1036; Beyotime) for 10 min at 37 °C. HUVECs cultured in 12-well plates were stained with Hoechst 33342 (C1028; Beyotime) for 10 min at 37 °C. Labeled THP-1 cells and HUVECs were washed three times with PBS. The THP-1 cells were then plated in HUVECs for a 4 h co-incubation in a 5% CO_2 atmosphere at 37 °C. After washing with PBS three times to remove the unadhered THP-1 cells, adhered THP-1 cells were counted from three randomly selected areas.

Cell viability assay
Cell viability was detected by using Cell Counting Kit-8 (CCK8, FD3788; Fdbio Science). First, HUVECs (0.5×10^4 cells/well) were seeded into 96-well plates and incubated overnight. Next, HUVECs were treated with LPS (either 0–1000 ng/mL for 24 h or 500 ng/mL for 0–24 h). Then 10 μL of CCK-8 reagent was added per well and the plates were incubated for 2 h in darkness at 37 °C. Finally, the absorbance was determined at 450 nm using PerkinElmer VICTOR 1420 (PerkinElmer, Templeton, MA, USA).

Immunohistochemistry assay
The tissues of human atherosclerotic plaques and normal arterial were sliced into 4 μm sections, dewaxed in xylene, and rehydrated. They were then incubated for 30 min in 10 mM citrate buffer for antigen retrieval, and the tissues were incubated with 3% H_2O_2 for 15 min at room temperature to eliminate endogenous peroxidase activity. Next, they were washed three times with PBS, blocked with 5% bovine serum albumin (abs9157; Absin, Shanghai, China) for 1 h, followed by incubation with EPSTI1 antibody (11627-1-AP, 1:100 dilution; Proteintech) at 4 °C overnight. Sections were then rinsed with PBS, incubated with enzyme-enhanced IgG Polymer anti-Rabbit IHC antibody (GK500705; Gene Tech, South San Francisco, CA, USA) for 30 min at room temperature and counter-stained with hematoxylin for 3 min. After washing three times with PBS, the results were observed using a microscope, and the expression of EPSTI1 was quantitated using ImageJ software.

Immunofluorescence assay
Sections were fixed in ice-cold acetone for 30 min, washed with PBS, and blocked with 10% goat serum for 1 h at room temperature, followed by incubation with CD31 antibody (MA3105, 1:100; InvivoGen) and EPSTI1 antibody (11627-1-AP, 1:100 dilution; Proteintech) at 4 °C overnight. Sections were rinsed with PBS, incubated with secondary antibodies for 1 h at room temperature, then mounted with flourished mounting medium with 4′,6-diamidino-2-phenylindole (DAPI). Images were captured by a Nikon A1R confocal microscope and analyzed using ImageJ.

Statistical analysis
Data were analyzed as the mean ± SD using GraphPad 8 software (GraphPad, San Diego, CA, USA). All experiments were repeated at least three times. The unpaired two-sided Student's *t*-test or one-way analysis of variance test was used to calculate *P* values. A value of $P < 0.05$ was considered statistically significant.

RESULTS

EPSTI1 is dramatically upregulated in human and mouse atherosclerotic plaques
To identify differentially expressed genes in atherosclerotic plaques, we have previously performed an expression microarray analysis of human aortic atherosclerotic plaques versus normal aortic tissues [17]. The results showed that EPSTI1 expression was significantly higher in atherosclerotic plaques than normal aortic tissues (Fig. 1a). qPCR analysis confirmed that the mRNA level of EPSTI1 was significantly upregulated in atherosclerotic plaques compared to normal aortic tissues (Fig. 1b). Consistently, both immunoblot and immunohistochemistry analyses showed EPSTI1 was elevated in human atherosclerotic plaques (Fig. 1c, d). It is well known that endothelial activation is a crucial step in the initiation of atherosclerosis [4]. Therefore, in order to further determine the endothelial expression of EPSTI1 in atherosclerotic plaques, we performed an immunofluorescence assay on human normal aortas and atherosclerotic plaques. As shown in Fig. 1e, double immunostaining of EPSTI1 and the endothelial cell marker CD31 demonstrated that the normal aortic intima was intact and smooth. EPSTI1 was mainly expressed in endothelial cells of the normal aortas. Furthermore, the expression of EPSTI1 in endothelial cells of atherosclerotic plaques was higher than that of the normal aortas. We also used mouse aortic root sections to confirm these findings in mouse models. As shown in Fig. 1f, the results showed that EPSTI1 was more expressed in endothelial cells than in smooth muscle cells of normal aortas. Together, these data demonstrate that EPSTI1 is markedly induced in endothelial cells of human and mouse atherosclerotic lesions, implying a potential involvement of EPSTI1 in atherosclerosis development.

EPSTI1 promotes THP-1 cell adhesion to HUVECs
Given that monocyte adhesion to endothelial cells is known to be the critical step in the initiation of atherosclerosis [18], we determined the effect of EPSTI1 on monocyte-endothelial cell adhesion by performing gain- and loss-of-function studies. On the one hand, HUVECs were transfected with EPSTI1 over-expressing or pcDNA-mock vector. Using qPCR and Western blot analyses, we confirmed the overexpression of EPSTI1 in HUVECs (Fig. 2a, b). To detect cell adhesion, we incubated the Dil-labeled THP-1 cells with Hoechst 33342-labeled HUVECs. The data showed that EPSTI1 overexpression significantly increased the number of THP-1 cells adhered to HUVECs (Fig. 2c). On the other hand, HUVECs were transfected with either negative control siRNA or siRNAs targeting EPSTI1 (siEPSTI1 #1, siEPSTI1 #2, and siEPSTI1 #3). The data demonstrated that EPSTI1 expression was effectively knocked down by EPSTI1 siRNAs, and the most effective one, siEPSTI1 #2, was selected for function assay (Fig. 2d, e). As expected, EPSTI1 deficiency significantly decreased the number of THP-1 cells adhered to HUVECs (Fig. 2f). In sum, these results suggest that EPSTI1 potentiates monocyte-endothelial cell adhesion.

EPSTI1 promotes THP-1 cell adhesion to endothelial cells by upregulating the expression of VCAM-1 and ICAM-1
We next sought to dissect how EPSTI1 affects monocyte-endothelial cell adhesion. It is well-known that VCAM-1 and ICAM-1 bind to monocyte cell-surface ligands and mediate monocyte rolling and firm adhesion [19]. We first detect the effect of EPSTI1 on the expression of VCAM-1 and ICAM-1 in HUVECs. As shown in Fig. 3a, b, EPSTI1 overexpression increased

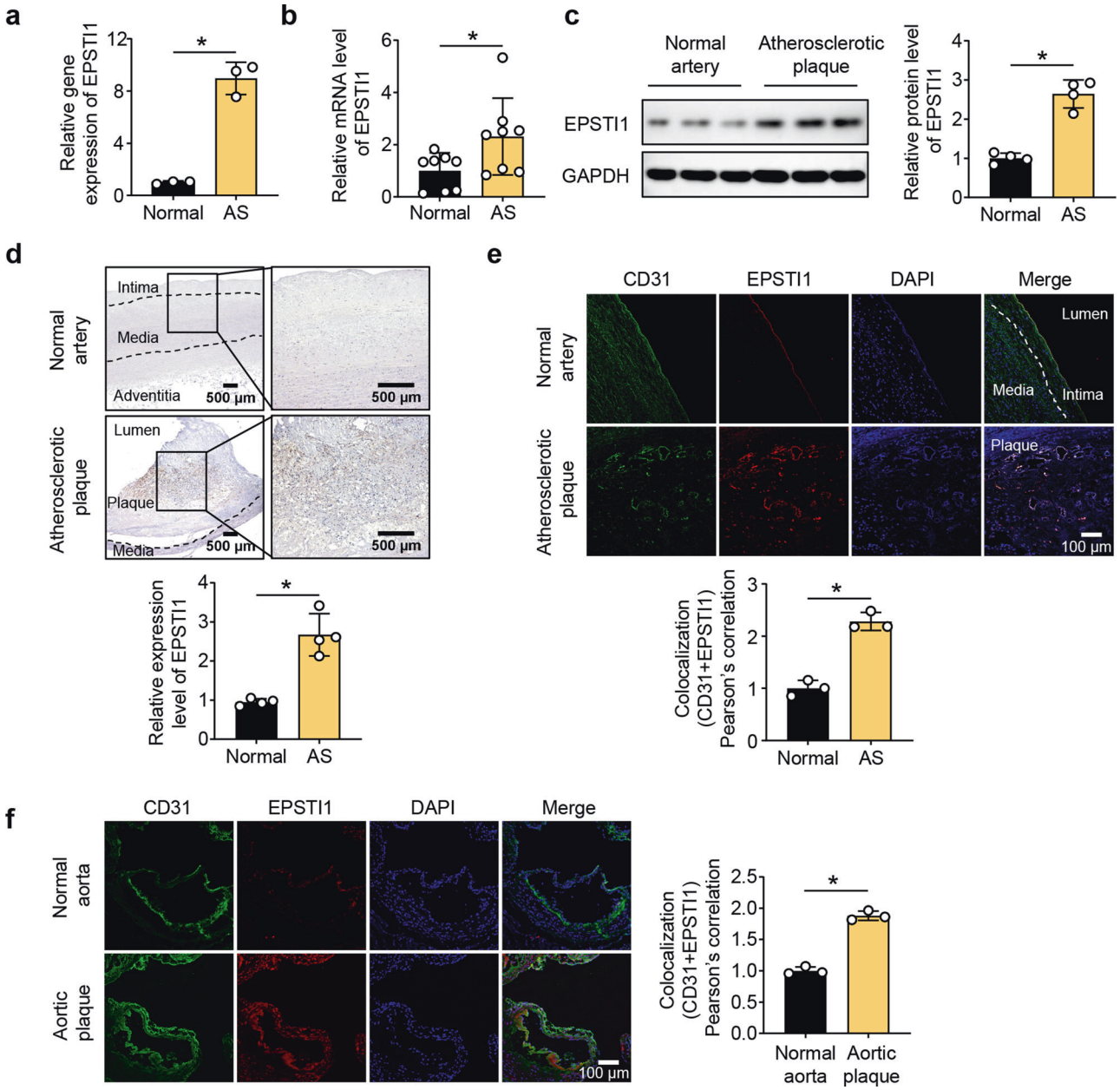

Fig. 1 EPSTI1 is dramatically upregulated in human and mouse atherosclerotic plaques. a RNA-seq analysis of EPSTI1 expression in human normal arteries and atherosclerotic plaques ($n = 3$). Normal: Normal arteries. AS: Atherosclerotic plaques. **b** qPCR analysis of EPSTI1 mRNA level in human normal arteries and atherosclerotic plaques ($n = 8$). **c** Western blot analysis of EPSTI1 protein level in human normal arteries and atherosclerotic plaques ($n = 4$). **d** Immunohistochemistry analysis of EPSTI1 protein level in human normal arteries and atherosclerotic plaques ($n = 4$). Scale bar: 500 μm. **e** Immunofluorescence assay of EPSTI1 expression in endothelial cells of human normal aortas and atherosclerotic plaques ($n = 3$). Scale bar: 100 μm. **f** Immunofluorescence assay of EPSTI1 expression in endothelial cells of normal aortas and aortic plaques in mice ($n = 3$). Scale bar: 100 μm. All data are expressed as mean ± SD. $^{*}P < 0.05$.

both mRNA and protein levels of VCAM-1 and ICAM-1 in HUVECs. In contrast, EPSTI1 knockdown by specific siRNA led to a decrease in VCAM-1 and ICAM-1 expression (Fig. 3c, d). We further asked whether VCAM-1 and ICAM-1 are required for EPSTI1-promoted THP-1 cell adhesion to endothelial cells. SiVCAM-1 #1 and siICAM-1 #2 were selected to knockdown VCAM-1 and ICAM-1, respectively, in the following experiments (Fig. 3e, f). Cell adhesion assay showed that EPSTI1 overexpression-increased THP-1 cell-endothelial cell adhesion could be partially reversed by siVCAM-1 #1 or siICAM-1 #2 transfection, while completely blocked by siVCAM-1 #1 and siICAM-1 #2 transfection (Fig. 3g). Together, these results demonstrate that EPSTI1 promotes monocyte adhesion to endothelial cells via the VCAM-1 and ICAM-1 upregulation.

EPSTI1 is involved in LPS-induced expression of VCAM-1 and ICAM-1 and monocyte-endothelial cell adhesion

LPS is a well-characterized vascular injury factor and increases VCAM-1 and ICAM-1 expression [20, 21]. Therefore, we explored whether LPS affects the EPSTI1 level. HUVECs were treated with serial dilutions of LPS (0–1000 ng/mL) for 24 h or with constant doses of LPS (500 ng/mL) for 0–24 h. Cell viability was significantly reduced with the treatment of 100, 500, and 1000 ng/mL of LPS (Fig. 4a), and the percentage of viable cells decreased at 6, 12, and

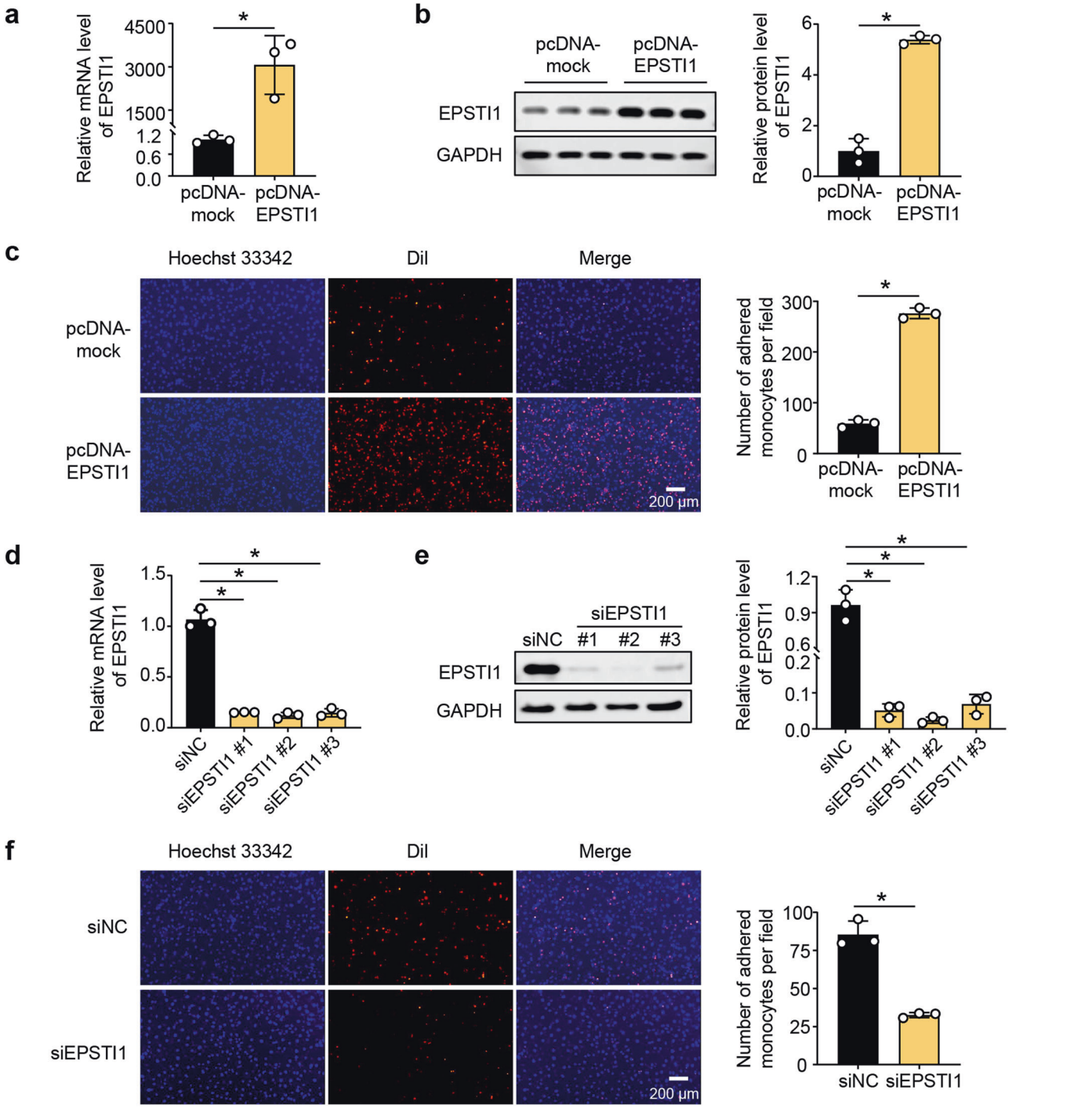

Fig. 2 EPSTI1 promotes THP-1 cell adhesion to HUVECs. a–c HUVECs were transfected with pcDNA-mock or pcDNA-EPSTI1 for 48 h. **a** qPCR analysis of EPSTI1 mRNA level ($n = 3$). **b** Western blot analysis of EPSTI1 protein level ($n = 3$). **c** Hoechst 33342-labeled HUVECs were incubated with DiI-labeled THP-1 cells for 4 h, and the adhesion of THP-1 cell to HUVECs was visualized by fluorescent microscopy ($n = 3$). Scale bar: 200 μm. **d**, **e** HUVECs were transfected with the siNC or siRNAs targeting EPSTI1 for 48 h. **d** qPCR analysis of EPSTI1 mRNA level ($n = 3$). **e** Western blot analysis of EPSTI1 protein level ($n = 3$). **f** HUVECs were transfected with siNC or siEPSTI1 #2 for 48 h. Hoechst 33342-labeled HUVECs were incubated with DiI-labeled THP-1 cells for 4 h, and the adhesion of THP-1 cell to HUVECs was visualized by fluorescence microscopy ($n = 3$). Scale bar: 200 μm. All data are expressed as mean ± SD. $^{*}P < 0.05$.

24 h (Fig. 4b). Our results were consistent with previous findings [22, 23]. qPCR and Western blot analyses revealed that LPS significantly upregulated the mRNA and protein levels of EPSTI1 (Fig. 4c–f). Furthermore, LPS significantly induced the expression of EPSTI1 after 6 h. The level of EPSTI1 peaked at 12 h and decreased at 24 h, but was still higher than the basic level. Consistent with previous findings [20, 24], LPS dramatically upregulated VCAM-1 and ICAM-1 mRNA and protein levels. Their expression peaked at 6 h, then declined and remained high (Fig. 4c–f). To dissect causal links between EPSTI1, VCAM-1 and ICAM-1, we treated EPSTI1-deficient HUVECs with LPS and determined the VCAM-1 and ICAM-1 expression. The data showed

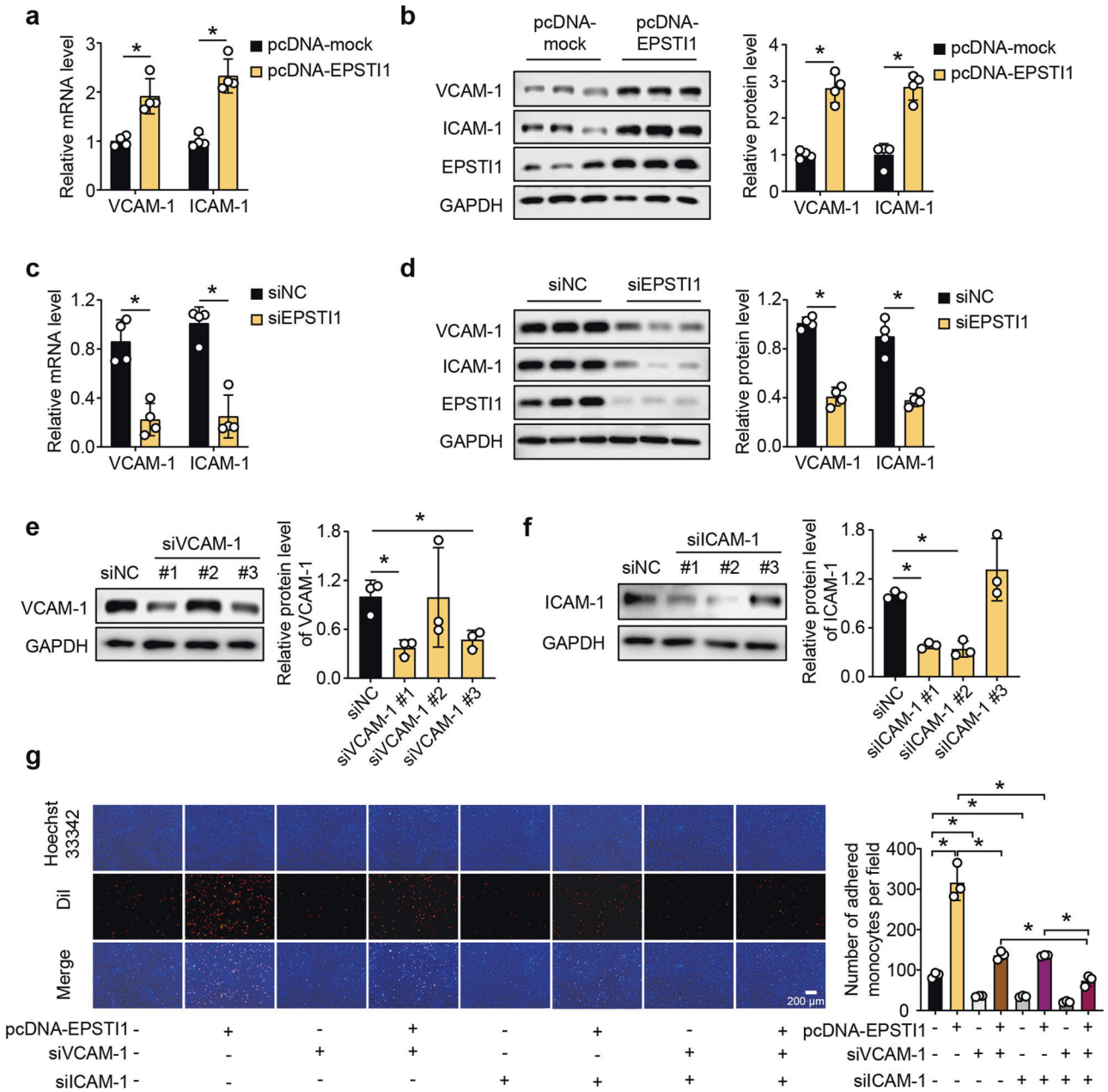

Fig. 3 EPSTI1 promotes THP-1 cell adhesion to endothelial cells by upregulating the expression of VCAM-1 and ICAM-1. a, **b** HUVECs were transfected with pcDNA-mock or pcDNA-EPSTI1 for 48 h. **a** qPCR analysis of VCAM-1 and ICAM-1 mRNA levels ($n = 4$). **b** Western blot analysis of VCAM-1 and ICAM-1 protein levels ($n = 4$). **c**, **d** HUVECs were transfected with siNC or siEPSTI1 #2 for 48 h. **(c)** qPCR analysis of VCAM-1 and ICAM-1 mRNA levels ($n = 4$). **(d)** Western blot analysis of VCAM-1 and ICAM-1 protein levels ($n = 4$). **e** HUVECs were transfected with siNC or siRNAs targeting VCAM-1 for 48 h, followed by Western blot analysis of VCAM-1 protein level ($n = 3$). **f** HUVECs were transfected with siNC or siRNAs targeting ICAM-1 for 48 h, followed by Western blot analysis of ICAM-1 protein level ($n = 3$). **g** HUVECs were transfected with pcDNA-mock or pcDNA-EPSTI1 for 24 h, and then transfected with siNC, siVCAM1 #1, or siICAM-1 #2. At a total of 48 h later, Hoechst 33342-labeled HUVECs were incubated with Dil-labeled THP-1 cells for 4 h, and the adhesion of THP-1 cell to HUVECs was visualized by fluorescence microscopy ($n = 3$). Scale bar: 200 μm. All data are expressed as mean ± SD. $^{*}P < 0.05$.

that EPSTI1 knockdown abolished LPS-induced upregulation of VCAM-1 and ICAM-1 (Fig. 4g, h). Additionally, LPS-increased THP-1 cell adhesion to HUVECs was negated by EPSTI1 loss (Fig. 4i). Taken together, we revealed that EPSTI1 mediates LPS-induced VCAM-1 and ICAM-1 upregulation and subsequently enhances THP-1 cell adhesion to HUVECs.

LPS induces the expression of EPSTI1 through p65

Since LPS rapidly activates p65 nuclear translocation, which strongly enhances the transcription of inflammatory factors and adhesion molecules [25], we finally asked whether p65 is involved in LPS-induced EPSTI1 expression. By transfecting p65 over-expressing plasmid, we found that p65 promoted both mRNA and protein levels of EPSTI1 (Fig. 5a, b). In contrast, p65 knock-downed by specific sip65 #1 (Fig. 5c, d) showed decreased expression of EPSTI1 (Fig. 5e, f). Consistent with previous findings [26, 27], LPS significantly induced p65 nuclear translocation in HUVECs (Fig. 5g). Furthermore, LPS-elevated EPSTI1 mRNA and protein levels were down-regulated by p65 deficiency (Fig. 5h, i). Collectively, these findings demonstrated a p65-dependent upregulation of EPSTI1 upon LPS treatment.

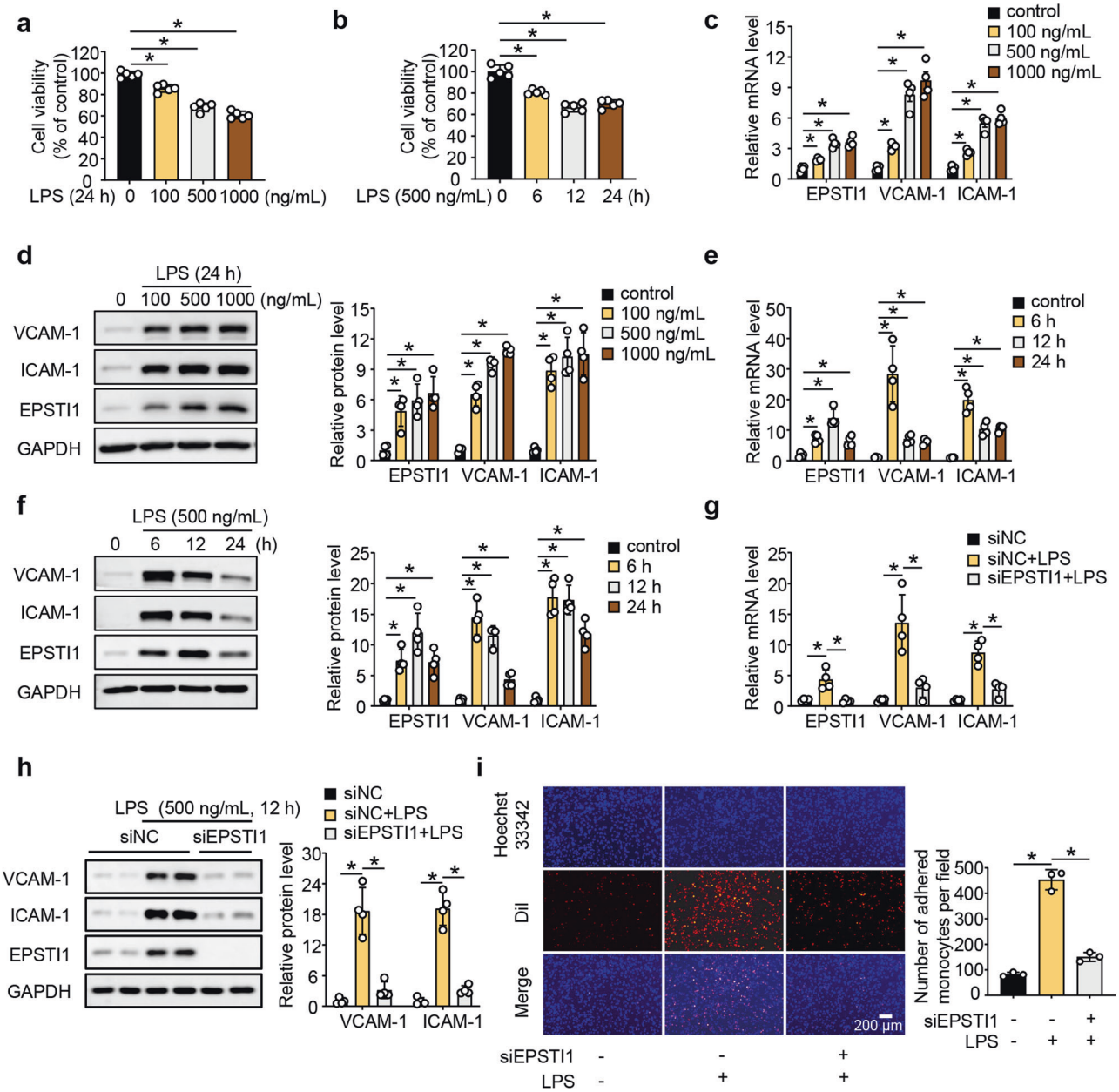

Fig. 4 EPSTI1 is involved in LPS-induced expression of VCAM-1 and ICAM-1 and monocyte-endothelial cell adhesion. a, **c**, **d** HUVECs were treated with 0, 100, 500, or 1000 ng/mL LPS for 24 h. **b**, **e**, **f** HUVECs were treated with 500 ng/mL LPS for 0, 6, 12, or 24 h. **a**, **b** Cell viability of HUVECs after treatment with LPS ($n = 5$). **c**, **e** qPCR analysis of EPSTI1, VCAM-1 and ICAM-1 mRNA levels ($n = 4$). **d**, **f** Western blot analysis of EPSTI1, VCAM-1 and ICAM-1 protein levels ($n = 4$). **g**–**i** HUVECs were transfected with siNC or siEPSTI1 #2 for 36 h and then treated with 500 ng/mL LPS for 12 h. **g** qPCR analysis of EPSTI1, VCAM-1 and ICAM-1 mRNA levels ($n = 4$). **h** Western blot analysis of EPSTI1, VCAM-1 and ICAM-1 protein levels ($n = 4$). **i** Hoechst 33342-labeled HUVECs were incubated with DiI-labeled THP-1 cells for 4 h, and the adhesion of THP-1 cell to HUVECs was visualized by fluorescence microscopy ($n = 3$). Scale bar: 200 μm. All data are expressed as mean ± SD. $^{*}P < 0.05$.

DISCUSSION

The present study discovers a significant increase in the EPSTI1 expression in endothelial cells of human and mouse atherosclerotic plaques and the effect of EPSTI1 on instigating monocyte-endothelial cell adhesion. We further found that EPSTI1 induces THP-1 cell adhesion to HUVECs by upregulating VCAM-1 and ICAM-1. EPSTI1 supports LPS-induced VCAM-1 and ICAM-1 expression and THP-1-endothelial cell adhesion. Finally, we revealed that LPS increases EPSTI1 via p65. Our findings suggest that EPSTI1 may be involved in atherogenesis (Fig. 6).

EPSTI1 has been widely reported to play an essential role in a variety of cellular behaviors in cancers, such as cell proliferation, migration, and invasion [14, 28, 29]. Recently, increasing studies have reported that EPSTI1 plays a vital role in the activation of immune responses in several chronic inflammatory diseases such as multiple sclerosis and systemic lupus erythematosus [30, 31]. Atherosclerosis is also regarded as a chronic inflammatory disease of the arterial wall [32]. We have previously reported the role of TM4SF19, and long non-coding RNAs, such as NEXN-AS1 and RP11-728F11.4, in the pathogenesis of atherosclerosis [33–35]. By analyzing our previous RNA-sequencing data performed in human atherosclerotic plaques [17], we found that EPSTI1 showed significantly higher expression in atherosclerotic plaques than normal aortic tissues. In addition, given that endothelial activation

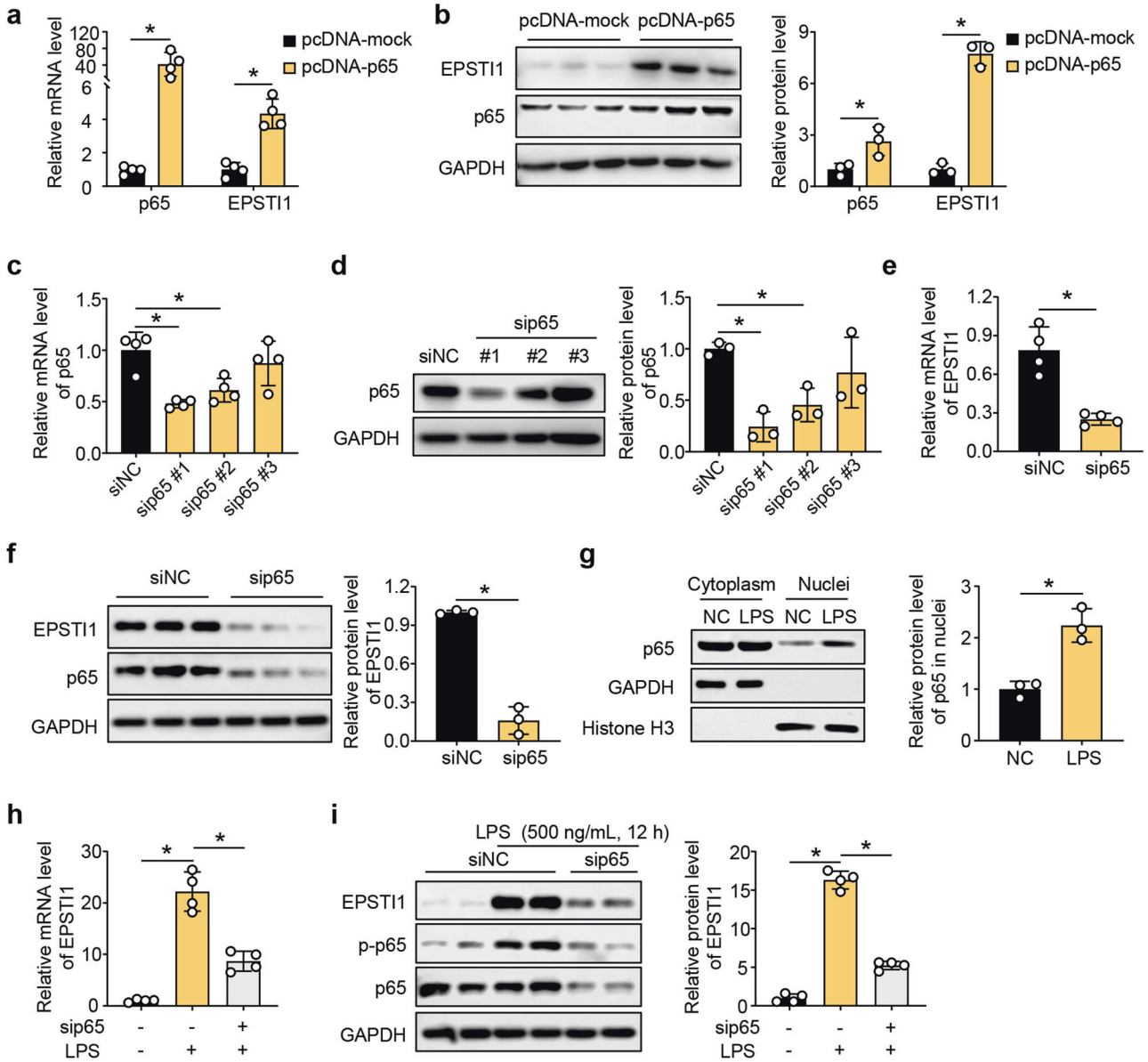

Fig. 5 LPS induces the expression of EPSTI1 through p65. a, **b** HUVECs were transfected with pcDNA-mock or pcDNA-p65 for 48 h. **a** qPCR analysis of p65 and EPSTI1 mRNA levels ($n = 4$). **b** Western blot analysis of p65 and EPSTI1 protein levels ($n = 3$). **c**, **d** HUVECs were transfected with the siNC or siRNAs targeting p65 for 48 h. **c** qPCR analysis of p65 mRNA level ($n = 4$). **d** Western blot analysis of p65 protein level ($n = 3$). **e**, **f** HUVECs were transfected with the siNC or sip65 #1 for 48 h. **e** qPCR analysis of EPSTI1 mRNA level ($n = 4$). **f** Western blot analysis of EPSTI1 protein level ($n = 3$). **g** Western blot analysis of p65 nuclear protein level of HUVECs after treatment with 500 ng/mL LPS for 12 h ($n = 3$). **h**, **i** HUVECs were transfected with the siNC or sip65 #1 for 36 h and then treated with 500 ng/mL LPS for 12 h. **h** qPCR analysis of EPSTI1 mRNA level ($n = 4$). **i** Western blot analysis of EPSTI1 protein level ($n = 4$). All data are expressed as mean ± SD. $^{*}P < 0.05$.

is a critical step in the initiation of atherosclerosis [4], we performed double immunostaining of EPSTI1 and the endothelial cell marker CD31 in human and mouse atherosclerotic plaques. And we found that EPSTI1 was dominantly expressed in endothelial cells of the normal aortas and the expression of EPSTI1 in endothelial cells of atherosclerotic plaques was higher than that of the normal aortas.

Although the occurrence of atherosclerosis is closely related to prolonged hyperlipidemia, it is increasingly clear that there is an immunological component to the progression of atherosclerosis, as indicated by the accumulation of leukocytes in atherosclerotic lesions [36, 37]. In fact, growing evidence suggests that the adhesion of circulating monocyte to vascular endothelial cells is an early step in the formation of atherosclerotic lesions [18, 38, 39]. Thus, determining the extent of monocyte-endothelial adhesion affected by EPSTI1 expression is critical to understanding the link between EPSTI1 and atherosclerosis. Notably, our results showed that EPSTI1 positively promoted THP-1 cell adhesion to HUVECs, suggesting that EPSTI1 may aggravate atherosclerosis by promoting monocyte recruitment into the intima, where the cells are exposed to hyperlipidemia, ingest lipids, and differentiate into macrophages, leading to the lipid plaque formation [33].

The recruitment and adhesion of circulating monocyte occur through a tightly regulated multi-step process mediated by monocytic integrins and the endothelial cell surface adhesion molecules [19, 40]. Studies have previously suggested that α4-integrin and β2-integrin, abundantly expressed on circulating monocyte, bind to endothelial VCAM-1 and ICAM-1, respectively, which are upregulated in activated endothelial cells, resulting in the firm adhesion of monocyte to endothelial cells [40, 41]. Consistent

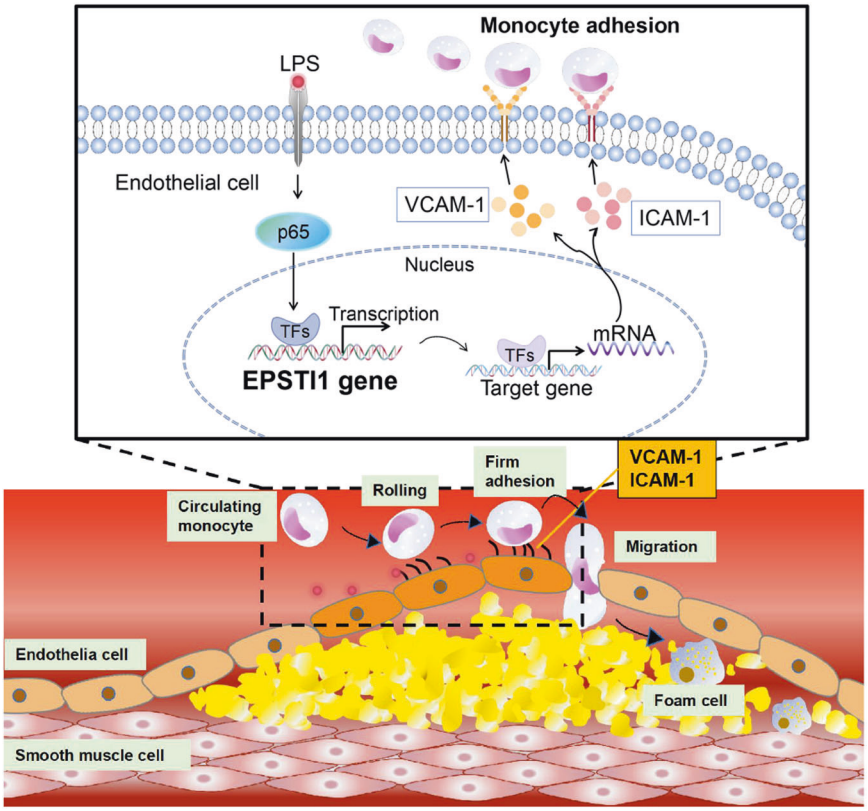

Fig. 6 Model of the EPSTI1 effects. By acting on HUVECs, LPS induces the expression of EPSTI1 through p65, and EPSTI1 further upregulates the expressions of VCAM-1 and ICAM-1, thereby promoting the circulating monocyte adhesion to endothelial cells.

with previous studies, we demonstrated that EPSTI1 promoted monocyte-endothelial cell adhesion via positively modulating VCAM-1 and ICAM-1 expression. Increasing studies have revealed that pre-treatment with anti-VCAM-1 and anti-ICAM-1 significantly lowered the recruitment of monocyte to the atherosclerotic plaque, as well as lesion size [42–44], suggesting that anti-EPSTI1 may relieve atherosclerosis by lowering the recruitment of monocyte to endothelial cells via VCAM-1 and ICAM-1 suppression, which needs further research in cell model and in vivo animal model of atherosclerosis. Since LPS is a known pro-atherogenic metabolite, which can promote the monocyte-endothelial cell adhesion via enhancing VCAM-1 and ICAM-1 expression [20, 45, 46], the well-established LPS-induced endothelial cells injured model was used in the current study. In line with previous findings [20, 22, 45], LPS significantly inhibited cell viability and induced VCAM-1 and ICAM-1 expression in a time- and concentration-dependent manner in HUVECs. Notably, EPSTI1 expression was also significantly induced by LPS in a time- and concentration-dependent manner at both mRNA and protein levels. Further studies revealed that knockdown of EPSTI1 not only reduced basal VCAM-1 and ICAM-1 expression, but also inhibited LPS-induced VCAM-1 and ICAM-1 expression. More importantly, knockdown of EPSTI1 significantly lowered the adhesion of THP-1 cell to HUVECs, raising the possibility that EPSTI1 could serve as a therapeutic target for monocyte-endothelial cell adhesion in atherosclerotic lesions. In addition, we also further investigated how LPS regulated EPSTI1 expression. It is well known that LPS induces activation of NF-κB p65, a central transcription factor, enabling its translocation to the nucleus where it activates the downstream gene transcription, including cell adhesion molecules and inflammation factor [25, 47, 48]. Since p65 is the most important downstream pathway in the LPS mediated signal transduction pathway, we further found that LPS induced EPSTI1 expression via p65.

The results of this study provide strong evidence for the effect of EPSTI1 on monocyte adhesion to endothelial cells. These findings provide new insights into the pathogenesis and treatment of atherosclerosis. However, several limitations of our study remain. Firstly, the mechanism by which EPSTI1 regulates VCAM-1 and ICAM-1 expression needs to be further investigated. Secondly, our experiments were majorly carried out in vitro in cells. Therefore, proper in vivo animal studies are required to verify our results.

In summary, our findings revealed the increased EPSTI1 expression in endothelial cells of atherosclerotic plaques and demonstrated the critical role of EPSTI1 in promoting monocyte adhesion to endothelial cells by enhancing VCAM-1 and ICAM-1 expression. Our study provides new insight into how circulating monocyte adhering to vascular endothelial cells is regulated by EPSTI1, suggesting it as a potential therapeutic target for adjusting monocyte-endothelial cell adhesion in atherosclerosis.

ACKNOWLEDGEMENTS

This work was supported by the National Natural Science Foundation of China (Grant numbers: 82072335, 81871701, 81974046, and 82170467), the Natural Science Fund of Guangdong Province (Grant numbers: 2020B1515020013 and 2018A030313533), Guangzhou Women and Children's Medical Center (Grant number: GWCMC2020-6-010).

AUTHOR CONTRIBUTIONS

XYD and YWH developed the study's concept, designed the experiments, and wrote the manuscript; YRB and SCZ conducted the experiments and acquired data; YS, MLT, KLZ, and RCH analyzed data; MJ, XHL, LMW, and SGW revised the manuscript.

ADDITIONAL INFORMATION

Competing interests: The authors declare no competing interests.

REFERENCES

1. Virani SS, Alonso A, Aparicio HJ, Benjamin EJ, Bittencourt MS, Callaway CW, et al. Heart disease and stroke statistics-2021 update: A report from the American heart association. Circulation. 2021;143:e254–e743.
2. Galkina E, Ley K. Immune and inflammatory mechanisms of atherosclerosis (*). Annu Rev Immunol. 2009;27:165–97.
3. Bonetti PO, Lerman LO, Lerman A. Endothelial dysfunction: a marker of atherosclerotic risk. Arterioscler Thromb Vasc Biol. 2003;23:168–75.
4. Gimbrone MA Jr., García-Cardeña G. Endothelial cell dysfunction and the pathobiology of atherosclerosis. Circ Res. 2016;118:620–36.
5. Meng B, Li Y, Ding Y, Xu X, Wang L, Guo B, et al. Myeloid-derived growth factor inhibits inflammation and alleviates endothelial injury and atherosclerosis in mice. Sci Adv. 2021;7:eabe6903.
6. Roth Flach RJ, Skoura A, Matevossian A, Danai LV, Zheng W, Cortes C, et al. Endothelial protein kinase MAP4K4 promotes vascular inflammation and atherosclerosis. Nat Commun. 2015;6:8995.
7. Bourdillon MC, Poston RN, Covacho C, Chignier E, Bricca G, McGregor JL. ICAM-1 deficiency reduces atherosclerotic lesions in double-knockout mice (ApoE (-/-)/ICAM-1(-/-)) fed a fat or a chow diet. Annu Rev Immunol. 2000;20:2630–5.
8. Ramos CL, Huo Y, Jung U, Ghosh S, Manka DR, Sarembock IJ, et al. Direct demonstration of P-selectin- and VCAM-1-dependent mononuclear cell rolling in early atherosclerotic lesions of apolipoprotein E-deficient mice. Circ Res. 1999;84:1237–44.
9. Nielsen HL, Rønnov-Jessen L, Villadsen R, Petersen OW. Identification of EPSTI1, a novel gene induced by epithelial-stromal interaction in human breast cancer. Genomics. 2002;79:703–10.
10. de Neergaard M, Kim J, Villadsen R, Fridriksdottir AJ, Rank F, Timmermans-Wielenga V, et al. Epithelial-stromal interaction 1 (EPSTI1) substitutes for peritumoral fibroblasts in the tumor microenvironment. Am J Pathol. 2010;176:1229–40.
11. Kim YH, Lee JR, Hahn MJ. Regulation of inflammatory gene expression in macrophages by epithelial-stromal interaction 1 (Epsti1). Biochem Biophys Res Commun. 2018;496:778–83.
12. Fan M, Arai M, Tawada A, Chiba T, Fukushima R, Uzawa K, et al. Contrasting functions of the epithelial-stromal interaction 1 gene, in human oral and lung squamous cell cancers. Oncol Rep. 2022;47:5.
13. Tan YY, Xu XY, Wang JF, Zhang CW, Zhang SC. MiR-654-5p attenuates breast cancer progression by targeting EPSTI1. Am J Cancer Res. 2016;6:522–32.
14. Rao C, Frodyma DE, Southekal S, Svoboda RA, Black AR, Guda C, et al. KSR1- and ERK-dependent translational regulation of the epithelial-to-mesenchymal transition. Elife. 2021;10:e66608.
15. Ishii T, Onda H, Tanigawa A, Ohshima S, Fujiwara H, Mima T, et al. Isolation and expression profiling of genes upregulated in the peripheral blood cells of systemic lupus erythematosus patients. DNA Res. 2005;12:429–39.
16. Sun JL, Zhang HZ, Liu SY, Lian CF, Chen ZL, Shao TH, et al. Elevated EPSTI1 promote B cell hyperactivation through NF-κB signalling in patients with primary Sjögren's syndrome. Ann Rheum Dis. 2020;79:518–24.
17. Hu YW, Guo FX, Xu YJ, Li P, Lu ZF, McVey DG, et al. Long noncoding RNA NEXN-AS1 mitigates atherosclerosis by regulating the actin-binding protein NEXN. J Clin Invest. 2019;129:1115–28.
18. Mestas J, Ley K. Monocyte-endothelial cell interactions in the development of atherosclerosis. Trends Cardiovasc Med. 2008;18:228–32.
19. Ley K, Laudanna C, Cybulsky MI, Nourshargh S. Getting to the site of inflammation: The leukocyte adhesion cascade updated. Nat Rev Immunol. 2007;7:678–89.
20. Yang B, Yang H, Lu X, Wang L, Li H, Chen S, et al. MiR-520b inhibits endothelial activation by targeting NF-κB p65-VCAM1 axis. Biochem Pharmacol. 2021;188:114540.
21. Hou X, Yang S, Yin J. Blocking the REDD1/TXNIP axis ameliorates LPS-induced vascular endothelial cell injury through repressing oxidative stress and apoptosis. Am J Physiol Cell Physiol. 2019;316:C104–C10.
22. Xiao Q, Zhu X, Yang S, Wang J, Yin R, Song J, et al. LPS induces CXCL16 expression in HUVECs through the miR-146a-mediated TLR4 pathway. Int Immunopharmacol. 2019;69:143–9.
23. Wu J, Li X, Huang L, Jiang S, Tu F, Zhang X, et al. HSPA12B inhibits lipopolysaccharide-induced inflammatory response in human umbilical vein endothelial cells. J Cell Mol Med. 2015;19:544–54.
24. Li M, Liu Y, Fu Y, Gong R, Xia H, Huang X, et al. Interleukin-35 inhibits lipopolysaccharide-induced endothelial cell activation by downregulating inflammation and apoptosis. Exp Cell Res. 2021;407:112784.
25. Prescott JA, Mitchell JP, Cook SJ. Inhibitory feedback control of NF-κB signalling in health and disease. Biochem J. 2021;478:2619–64.
26. Chen X, Xiu M, Xing J, Yu S, Min D, Guo F. Lanthanum chloride inhibits LPS mediated expressions of pro-inflammatory cytokines and adhesion molecules in HUVECs: Involvement of NF-κB-Jmjd3 signaling. Cell Physiol Biochem. 2017;42:1713–24.
27. Gao A, Wang Y, Gao X, Tian W. LCZ696 ameliorates lipopolysaccharide-induced endothelial injury. Aging. 2021;13:9582–91.
28. Capdevila-Busquets E, Badiola N, Arroyo R, Alcalde V, Soler-López M, Aloy P. Breast cancer genes PSMC3IP and EPSTI1 play a role in apoptosis regulation. PLoS One. 2015;10:e0115352.
29. Li T, Lu H, Shen C, Lahiri SK, Wason MS, Mukherjee D, et al. Identification of epithelial stromal interaction 1 as a novel effector downstream of Krüppel-like factor 8 in breast cancer invasion and metastasis. Oncogene. 2014;33:4746–55.
30. Sol N, Leurs CE, Veld SGI, Strijbis EM, Vancura A, Schweiger MW, et al. Blood platelet RNA enables the detection of multiple sclerosis. Mult Scler J Exp Transl Clin. 2020;6:2055217320946784.
31. Zhao X, Zhang L, Wang J, Zhang M, Song Z, Ni B, et al. Identification of key biomarkers and immune infiltration in systemic lupus erythematosus by integrated bioinformatics analysis. J Transl Med. 2021;19:35.
32. Soehnlein O, Libby P. Targeting inflammation in atherosclerosis - from experimental insights to the clinic. Nat Rev Drug Discov. 2021;20:589–610.
33. Wu LM, Wu SG, Chen F, Wu Q, Wu CM, Kang CM, et al. Atorvastatin inhibits pyroptosis through the lncRNA NEXN-AS1/NEXN pathway in human vascular endothelial cells. Atherosclerosis. 2020;293:26–34.
34. Dong XH, Lu ZF, Kang CM, Li XH, Haworth KE, Ma X, et al. The long noncoding RNA RP11-728F11.4 promotes atherosclerosis. Arterioscler Thromb Vasc Biol. 2021;41:1191–204.
35. Ding L, Li LM, Hu B, Wang JL, Lu YB, Zhang RY, et al. TM4SF19 aggravates LPS-induced attenuation of vascular endothelial cell adherens junctions by suppressing VE-cadherin expression. Biochem Biophys Res Commun. 2020;533:1204–11.
36. Galkina E, Ley K. Leukocyte influx in atherosclerosis. Curr Drug Targets. 2007;8:1239–48.
37. Wezel A, van der Velden D, Maassen JM, Lagraauw HM, de Vries MR, Karper JC, et al. RP105 deficiency attenuates early atherosclerosis via decreased monocyte influx in a CCR2 dependent manner. Atherosclerosis. 2015;238:132–9.
38. Riopel M, Vassallo M, Ehinger E, Pattison J, Bowden K, Winkels H, et al. CX3CL1-Fc treatment prevents atherosclerosis in Ldlr KO mice. Mol Metab. 2019;20:89–101.
39. Cui XB, Luan JN, Dong K, Chen S, Wang Y, Watford WT, et al. RGC-32 (Response Gene to Complement 32) deficiency protects endothelial cells from inflammation and attenuates atherosclerosis. Arterioscler Thromb Vasc Biol. 2018;38:e36–e47.
40. Woollard KJ, Geissmann F. Monocytes in atherosclerosis: subsets and functions. Nat Rev Cardiol. 2010;7:77–86.
41. Galkina E, Ley K. Vascular adhesion molecules in atherosclerosis. Arterioscler Thromb Vasc Biol. 2007;27:2292–301.
42. Arita-Okubo S, Kim-Kaneyama JR, Lei XF, Fu WG, Ohnishi K, Takeya M, et al. Role of Hic-5 in the formation of microvilli-like structures and the monocyte-endothelial interaction that accelerates atherosclerosis. Cardiovasc Res. 2015;105:361–71.
43. Patel SS, Thiagarajan R, Willerson JT, Yeh ET. Inhibition of alpha4 integrin and ICAM-1 markedly attenuate macrophage homing to atherosclerotic plaques in ApoE-deficient mice. Circulation. 1998;97:75–81.
44. Nageh MF, Sandberg ET, Marotti KR, Lin AH, Melchior EP, Bullard DC, et al. Deficiency of inflammatory cell adhesion molecules protects against atherosclerosis in mice. Arterioscler Thromb Vasc Biol. 1997;17:1517–20.
45. Hortelano S, López-Fontal R, Través PG, Villa N, Grashoff C, Boscá L, et al. ILK mediates LPS-induced vascular adhesion receptor expression and subsequent leucocyte trans-endothelial migration. Cardiovasc Res. 2010;86:283–92.
46. Rafiee L, Hajhashemi V, Javanmard SH. Maprotiline inhibits LPS-induced expression of adhesion molecules (ICAM-1 and VCAM-1) in human endothelial cells. Res Pharm Sci. 2016;11:138–44.
47. Collins T, Read MA, Neish AS, Whitley MZ, Thanos D, Maniatis T. Transcriptional regulation of endothelial cell adhesion molecules: NF-kappa B and cytokine-inducible enhancers. FASEB J. 1995;9:899–909.
48. Sun SC. The non-canonical NF-κB pathway in immunity and inflammation. Nat Rev Immunol. 2017;17:545–58.